MAXIMUM POWER POINT TRACKING ALGORITHM FOR PHOTOVOLTAIC SYSTEM USING SUPERVISED ONLINE COACTIVE NEURO FUZZY INFERENCE SYSTEM

T.Thamizhselvan
Asistant Professor / EEE, Rajalakshmi Engineering College, Chennai -602105, Tamilnadu state, India
Dr.R.Seyezhai
Associate Professor / EEE, SSN College of Engineering, Chennai, Tamilnadu, India.
Dr.K.Premkumar
Associate Professor / EEE, Rajalakshmi Engineering College, Chennai -602105, Tamilnadu state, India

Abstract: *Photovoltaic system normally requires maximum power point tracker as its output varies based on solar irradiance and temperature. In order to extract maximum power from PV, a supervised online coactive neuro fuzzy inference system based Maximum Power Point Tracking Technique (MPPT) is proposed in this paper. This MPP controller is executed in a soft switched IBC and it is compared with the conventional P&O and Fuzzy MPPT in terms of maximum power ratio, transient time, overshoot. In order to validate the effectiveness of the proposed MPPT control, two set of operating conditions are taken for analysis such as constant irradiance and step varying irradiance. The overall system is modeled using MATLAB / simulink Toolbox. Finally, the proposed supervised online CANFIS based MPPT is executed using DSP processor and the simulation results are verified experimentally.*

Keywords: *Photovoltaic system, MPPT, CANFIS,IBC and irradiance.*

1. Introduction

In the current scenario, as the population is increasing day by day, the electrical power demand is also increasing, but the conventional sources such as coal, diesel and gas are depleting. The need for renewable energy source becomes vital in this context. Many renewable energy technologies today are reliable, well developed and cost competitive with the conventional fuel generators. The cost of renewable energy technologies is on a falling trend as demand and production increases and the study of various alternate sources have gained momentum [1].

Among the renewable sources, Photovoltaic (PV) generation is important as it offers a lot of advantages such as low fuel costs, less pollutant, minimum maintenance and no noise [2]. Applications of PV have been widely employed for power generation, satellite power system, solar vehicle and solar battery charging stations. The major drawback of PV is the low efficiency of energy conversion when compared with other alternative resources. PV is a non-linear source that depends on irradiation and temperature in its process. Maximum power point tracking (MPPT) is developed to pull out the maximum power from the PV array [3-7].

In the literature, perturb and observe (P&O) algorithm is the most accepted and used extensively since it is the simplest algorithm and easy to implement when compared with other methods [8-11]. Moreover, it has some drawbacks such as poor tracking of maximum power due to abruptly change in irradiance, produces an oscillation around the maximum power point at low irradiance level, due to this it is unable to extract maximum power and response time of this algorithm is very slow. Another important drawback of this algorithm is its incapability to perform well in noisy environment. In such PV system, noise factor exists and must critically be measured as these have imperative effect on the decisions executed by the MPPT algorithm.

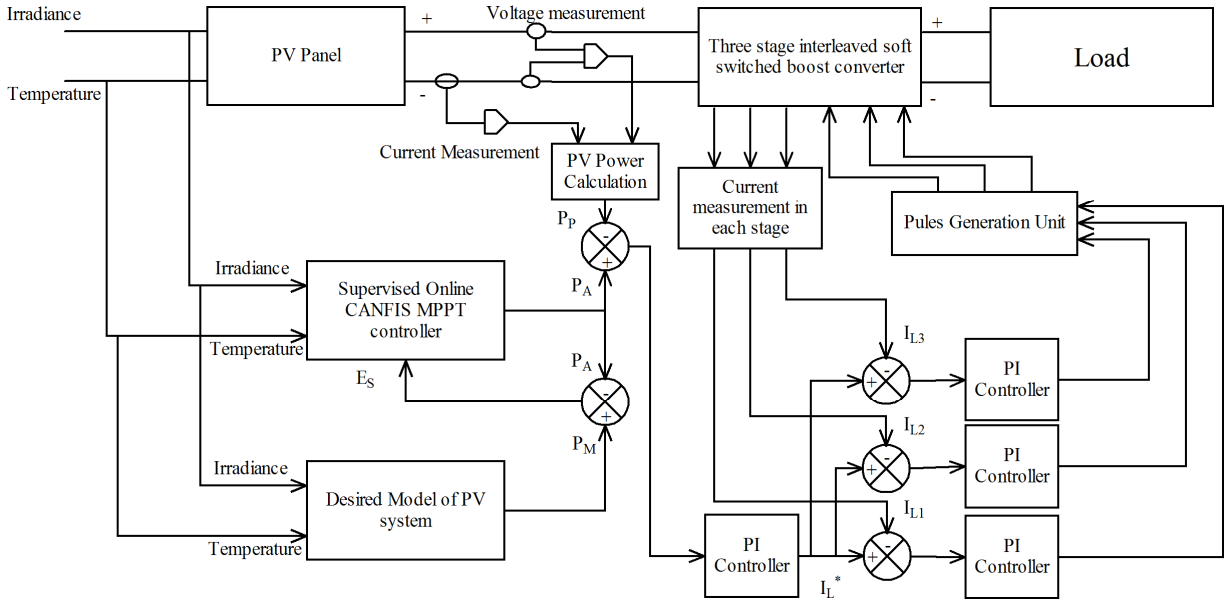

Fig. 1. Block diagram of Supervised online Coactive Neuro Fuzzy inference System based MPPT for PV system

Recently, artificial intelligence such as fuzzy logic, neural network and ANFIS based MPPT algorithms have been developed for PV system [12-13]. The advantages of using these methods are quick response time and more stable when compared to the traditional algorithms. Adaptive neuro fuzzy inference system is the most accepted among them because it is simple and realistic to be implemented. It has been implemented with significant improvement in efficiency.

ANFIS algorithm is superior when compared with Fuzzy logic and P&O algorithm, but it does not locate accurate maximum power point. Because, ANFIS control is trained in offline mode. There is a problem in offline training, as it requires large amount of representative input and output data.Training process is a timing consuming process, during training phase, some of the input and output data are not trained in this algorithm and it leads to decision making problem in maximum power point tracking.

To overcome the above mentioned drawbacks, a supervised online coactive neuro fuzzy inference system based MPPT algorithm is presented in this paper for improving maximum power point tracking performance of the PV system. The proposed control scheme consists of current balance control and MPPT control. Figure 1 shows the block diagram of the entire PV system. The maximum power point (MPP) power is calculated by the proposed MPPT using detected irradiance and temperature. Calculated MPP power is compared with the measured power from PV panel and used as an input of the power controller i.e., PI controller. The output of the power controller is used as a current reference for the next stage. The current reference is divided by the number of stage. This current reference is compared with the current of each stage, and the current error is used as an input of current controller. The gate signal for interleaved soft switched boost converter is generated by comparing the carrier signal and the output of the current controller. The proposed MPPT algorithm is analyzed and compared with the conventional P&O [11] and Fuzzy Logic algorithms [12] under different irradiance conditions. A prototype of the IBC is built and the proposed MPPT algorithm is tested and the results are validated.

The paper is organized as follows: mathematical modeling of PV array is presented in section 2. Basic operation of soft switched interleaved boost converter is presented in section 3 and supervised online coactive neuro fuzzy inference system based MPPT is presented in section 4. Simulation results are presented in section 5 and section 6 discusses experimental results. Concluding remarks is outlined in Section 7.

2. Mathematical model for a PV array

The equivalent circuit model of PV cell is shown in Figure 2 and the current flow through the diode can be expressed by Shockley's diode equation as,

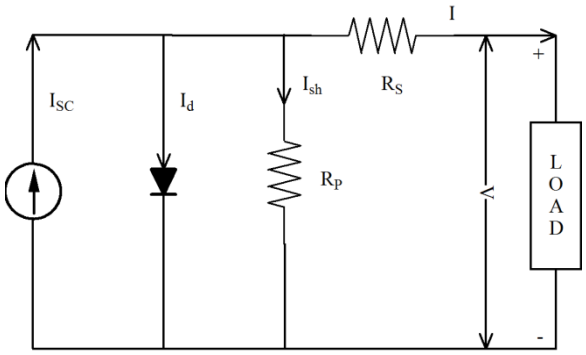

Fig.2. Equivalent circuit of PV cell

$$I_d = I_s\left(e^{\frac{q(V+IR_S}{AkT_C}} - 1\right) \quad (1)$$

Where,

I_S - The diode reverse saturation current (Amps),

V - The solar cell output voltage (Volt),

q - The charge of one electron, T_c -the solar cell temperature in Kelvin, *k* -Boltzmann constant

A - The junction perfection factor, which determines the diode deviation from the ideal p-n junction.

Current I_{SC} in Figure 2 indicates the photocurrent and it is dependent upon the light spectrum and the spectral response of the solar cell. The latter is according to the number of electron-hole pairs collected per incident photon, and thus depends on the optical absorption coefficient and diffusion length of the charge carriers [14]. The dependence of the photocurrent on the irradiance and cell temperature can be expressed by the following empirical equation,

$$I_{SC} = \{I_{SCR} + k_i(T_c - T_r)\}\frac{G}{100} \quad (2)$$

Where,

I_{SCR} - the short-circuit current generated at "T_r" which is the reference temperature in Kelvin.

k_i - The temperature coefficient of the short-circuit current and *G* -The irradiance in W/m^2.

Reverse saturation current (I_S) is correlated to temperature. Higher temperature raises the concentration of the intrinsic charge carriers and as a result results in higher carrier recombination. As a result rising temperature raise the reverse saturation current:

$$I_S = I_{or}\left(\frac{T_c}{T_r}\right)^3 e^{\left\{\frac{qE_g}{kA}\left[\frac{1}{T_r}-\frac{1}{T_c}\right]\right\}} \quad (3)$$

Where, I_{or} - The diode reverse saturation current at T_r and E_g - The band gap energy.If Nominal Operating Cell Temperature (NOCT) is given T_c is defined as

$$T_C - T_a = \frac{NOCT-20}{0.8}G \qquad \frac{kW}{m^2} \quad (4)$$

However a basic form can be used as,

$$T_C = T_a + 0.2 \times G \quad (5)$$

Taking into account the internal resistance R_P and R_S, we have the cell current expressed as

$$I = I_{SC} - I_S\left(e^{\left[\frac{q(V+IR_S)}{AkT_C}\right]} - 1\right) - \frac{V+IR_S}{R_P} \quad (6)$$

The above model can be extended to characterize PV array with N_p cells in parallel and N_s cell in series so we have,

$$I\left(1+\frac{R_{ST}}{R_{ShT}}\right) = n_pI_{SC} - n_pI_s\left(e^{\left[\frac{q\left(\frac{V}{n_s}+IR_{ST}\right)}{AkT_C}\right]} - 1\right) - \frac{V/n_s}{R_{ShT}} \quad (7)$$

Where,

$$R_{ShT} = \frac{n_p}{n_s} \times R_P \quad and \quad R_{ST} = \frac{n_s}{n_p} \times R_s$$

The above model illustrates that an array of PV cells is a nonlinear device having its characteristics depending on the solar irradiance and ambient temperature [15-16]. And power output of the PV array is given by,

$$P_{PV} = I \times V \quad (8)$$

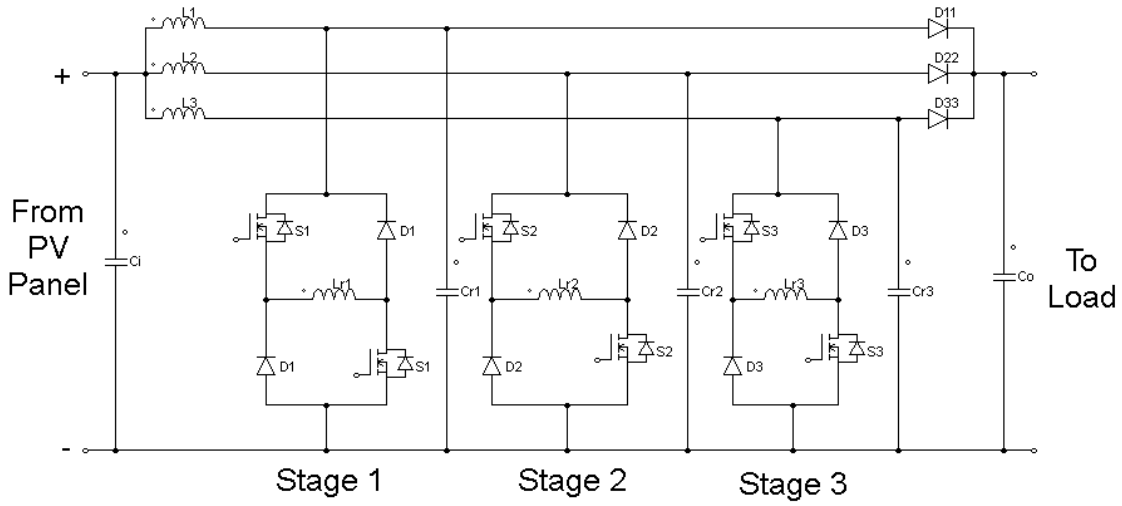

Fig.3(a). Three stages interleaved soft switched boost converter

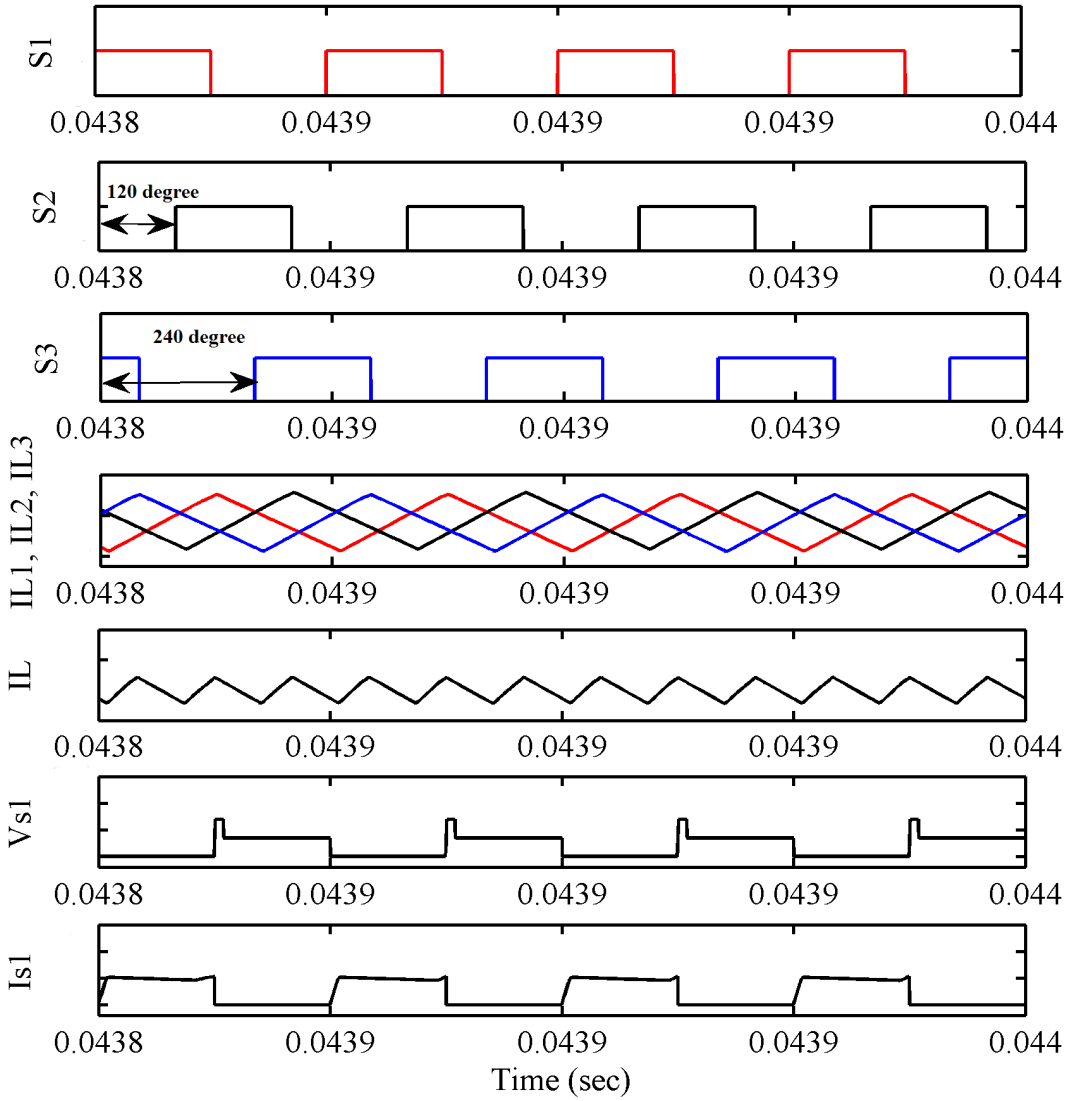

Fig.3(b). Switching logic of three stages interleaved soft switched boost converter

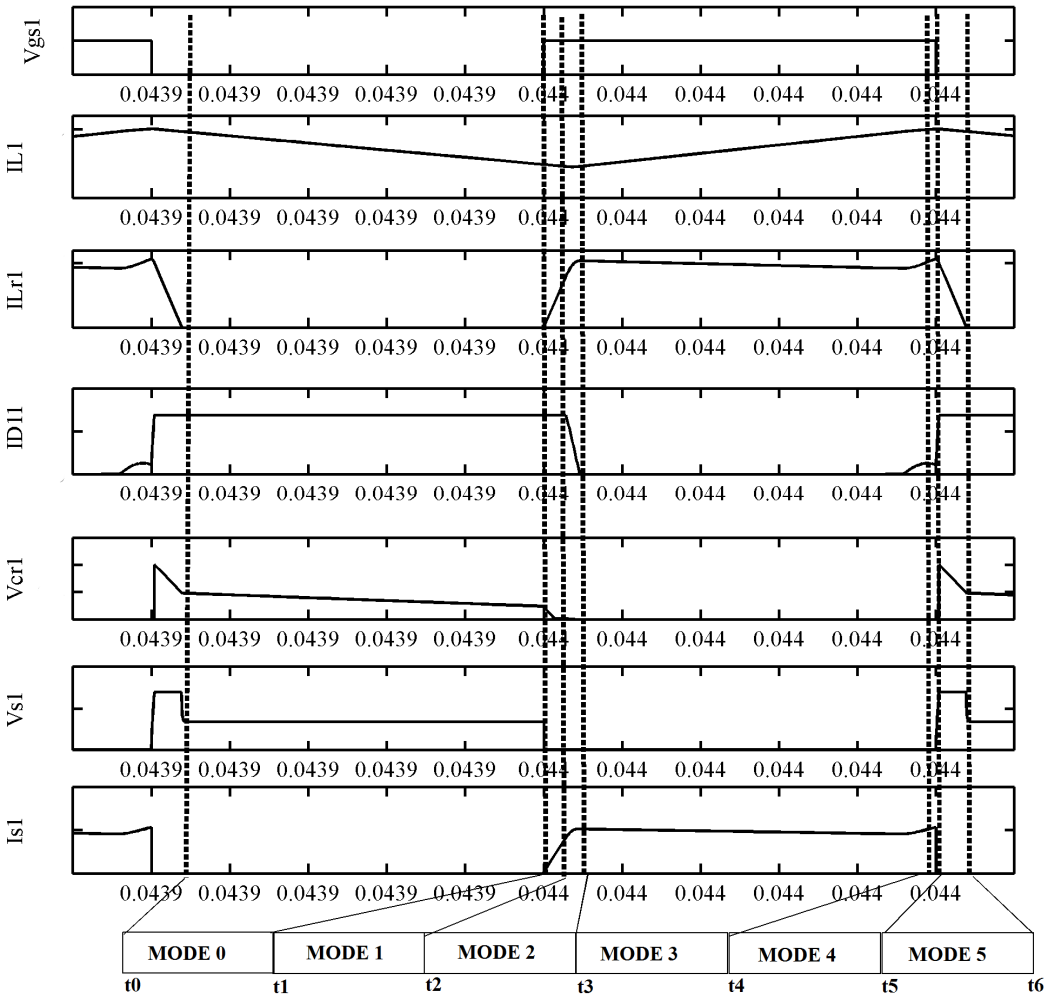

Fig.3(c). Mode of operation of three stage interleaved soft switched boost converter

3. Interleaved soft switched boost converter

DC-DC boost converters are employed as interfacing circuit for the PV array with MPPT control to provide maximum power to the load [17]. Boost converter have simple topology, high power density, fast transient response and continuous input current and hence, this topology is used for different power electronics applications such as active PFC (power factor correction), photovoltaic power systems and fuel cells [18]. To provide high output voltage, dc- dc converter need to be operated at extreme duty cycle which subjects the switching devices to short pulse, high amplitude current which leads to reverse recovery and EMI (Electro Magnetic Interference) problems and the extreme duty cycle leads to poor dynamic response for line and load variations. Converters with coupled inductor can provide a high output voltage, less switching voltage loss without extreme duty cycle. But the leakage energy loss in the coupled inductor reduces the efficiency of the converter. To overcome these difficulties and to improve the performance of the boost converter interleaving technique can be used [19]. The benefits of interleaving include, reduced RMS current in the input capacitors, ripple current cancellation in the output capacitor, improved transient response and reduced EMI. In this paper, three stage interleaved soft switched boost converter is used to track the maximum power from PV system.

Figure 3(a) shows the three stage interleaved soft switched boost converter with soft switching that consists of auxiliary switches (S_1, S_2 and S_3), resonant diodes (D_1, D_2 and D_3), resonant inductors (L_{r1}, L_{r2} and L_{r3}) and resonant capacitors (C_{r1}, C_{r2} and C_{r3}). Three stages interleaving technique needs each boost converter to be connected in parallel and it is operated at the same switching frequency, and that the switch of each boost converter be phase-shifted

by 360°/3. Due to these features, the current ripple in source, voltage ripple at output and size of the passive components can be reduced. Due to the interleaving structure, the switching losses are reduced drastically compared to the conventional converter [20]. Further, zero voltage and zero current switching are employed for auxiliary switching devices to further reduce the switching losses. Consequently, this three-stage interleaved soft switched boost converter has the advantages of both the interleaving topology and soft switching cells.

Figure 3(b) shows the switching logic with the theoretical current and voltage waveforms. Two switches of each stage, such as (S_1, S_2 and S_3) are switched on and off, concurrently. Each phase has a phase shift of 120 degrees. Thus, the inductor current of each stage linearly rises or falls with a phase difference of 120 degrees with respect to the switching logic. As seen in Figure 3(b), the input current ripple is reduced and the input current ripple frequency becomes 3 times higher than the switching frequency. The modes of operation of the interleaved soft switched boost converter are divided into six modes .Figure 3(c) shows the modes of operation of the converter during one switching period.

During mode-0, switches (S_1, S_3) are in the off state and switch S_2 on state. The main inductor current (I_{Ll}, I_{L3}) flows to the load through the main diode (D_{11}, D_{33}) and reduces linearly. The main inductor current I_{L2} flows to the load through the main diode D_{22} and raises linearly. In mode-1, switches (S_1) is turned on with Zero Current Switching, due to the resonant inductor L_{r1}. The resonant inductor current (I_{Lr1}) starts to rise linearly. This mode is finished when I_{Lr1} has become equal to I_{L1}. Switch S_3 already conducting and switch S_2 is in off state during this mode. Mode 2 is known as a resonant mode. The diode (D_{11}) at output end is turned off. L_{r1} and the resonant capacitor (C_{r1}) start to resonate. The resonant capacitor voltage (V_{cr1}) reduces resonantly from the output voltage V_0 to zero.

During mode-3, the resonant diode (D_1) is turned on. I_{Lr1} flows through the two freewheeling paths, S_1 to L_{r1} to D_1 and S_1 to D_1 to L_{r1}. The I_{L1} starts to rise linearly and the path of the I_{L1} to L_1 to S_1 to L_{r1} to S_1. The V_{cr1} retains zero voltage.Mode-4 begins when S_1 is switched off with Zero Voltage Switching, due to capacitor voltage V_{cr1}. L_{r1} and C_{r1} start to resonate. The I_{Lr1} reduces resonantly and V_{cr1} starts to rise resonantly from zero to V_0. In mode-5, I_{L1} and I_{Lr1} are summed together and the resultant current flows to the output through D_{11}. I_{Lr1} reduces to zero during this mode; it is completed as I_{Lr1} has become equal to zero.

4. Supervised online coactive neuro fuzzy inference system based MPPT algorithm

Supervised learning techniques are more powerful in machine learning than unsupervised techniques because the availability of labeled training data that provides the clear standards for optimization model. Supervised learning of CANFIS structure can be formed using off line mode and online mode. Both operations have two types of learning i.e., structure learning and parameter learning. Structure learning is primarily to extract the fuzzy logic rules of the input data with tuning of fuzzy partitions for the input and output spaces. And so, the parameter learning adjusts the parameter of each pattern. These two forms are completed sequentially in off line operation. In the first stage, input data is partitioned and in a second phase, premises and consequent parameter of the network is updated using the gradient descent method and recursive least square method respectively [21].

The primary drawback of this sequential learning scheme of off-line operation is that, it requires large quantities of representative data collection in advance and also the independent realization of the structure system and parameter learning usually requires a great deal of time. To address these problems and for faster learning, online operation has been brought in to perform the structure learning and parameter learning phases concurrently. To enhance the performance still further, supervised online learning of CANFIS controller is proposed in this paper. The proposed supervised online Coactive Neuro Fuzzy Inference System combines the merits of neural network and fuzzy inference system. Moreover, it performs the structure and parameter learning phases simultaneously. The structure of supervised online learning of CANFIS controller is shown in Figure 4(a).

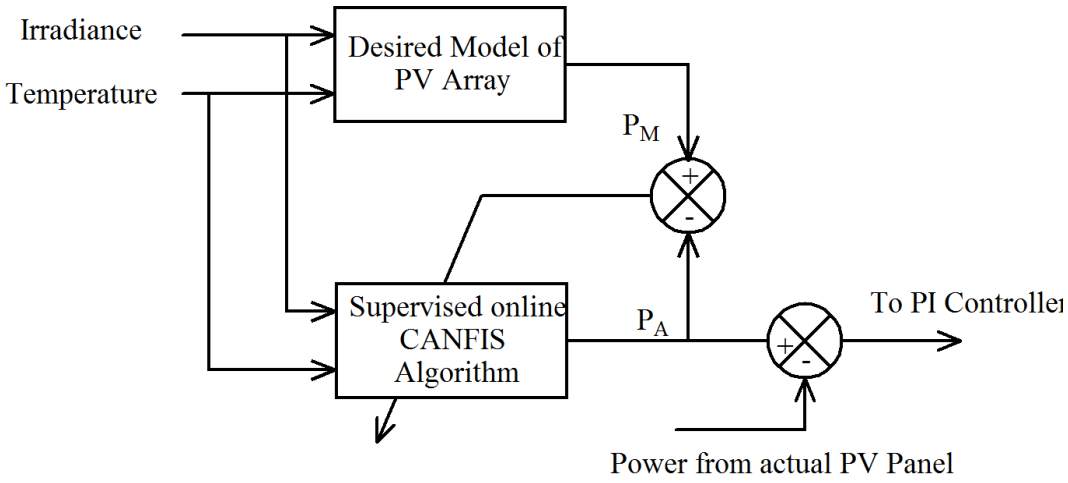

Fig.4(a). Structure of supervised online CANFIS based MPPT controller

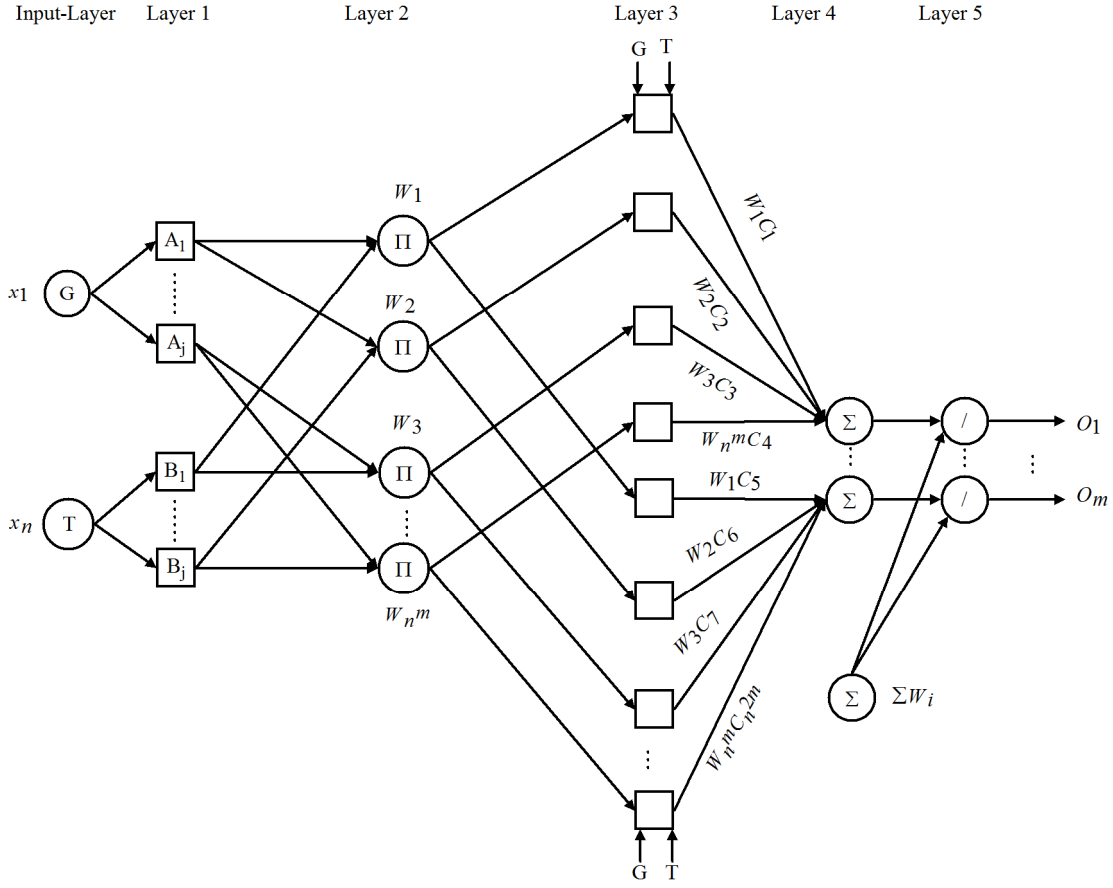

Fig.4. (b). Architecture of CANFIS Network

The output of the desired model provides the supervised output for the online CANFIS controller. The error between supervised output and online CANFIS controller output is given by

$$E_P = P_M - P_A \quad (9)$$

Next, the process of applying online learning algorithm to identify CANFIS parameters has been discussed. The CANFIS system, as the name suggests, is a Coactive Neuro-fuzzy inference machine. It also eliminates the shortcomings of the neural network and fuzzy logic system and it works as a universal approximator [21]. The CANFIS

controller consists of five layers as shown in Figure 4(b).

Initially, there is one input and output node in the CANFIS but rules in the CANFIS have been generated without any input and output membership function. The structure learning is used to find proper fuzzy logic rules from the input data and to minimize the number of rules and fuzzy sets generated on the universe of discourse of each input variable. The first step in the structure learning is to determine whether or not to perform the structure learning. If $G_{min} \leq G$ or $T_{min} \leq T$, where G_{min} and T_{min} are preset positive constants (irradiance and temperature), then the structure learning is necessary. Next, it will further decide whether or not to add a new membership function node, the associated fuzzy logic rule in the rule layer of the CANFIS. The parameter learning is based on supervised learning algorithms to adjust the parameter of the membership function, and parameter of the consequent part using the back propagation algorithm and recursive least square method respectively. Details of the parameter learning (back propagation and recursive least square algorithm) are explained in the layer 1 and layer 4 of the CANFIS [21].

Layer 1 is known as the input layer. In this layer input fuzzification takes place. Each input is assigned a membership value to each fuzzy subset that comprises that input's universe of discourse. Mathematically, this function can be expressed by equation (10),

$$O_{ij}^{(1)} = \mu_j\left(I_i^{(1)}\right) \tag{10}$$

Where O_{ij}^{1} is the layer 1 node's output, which matches to the j^{th} linguistic term of the i^{th} input variable I_i^{1}. A generalized Gaussian function memberships functions used for input variables and expressed in equation (11) as,

$$\mu_j(x_i) = \frac{1}{1+\left|\frac{x_i - c_{ij}}{a_{ij}}\right|^{b_{ij}}} \tag{11}$$

Where i=1…n and j=1…N_i (y=N_i). Numbers of input variables are equal to n and y is equal to number of fuzzy subsets for each input variable. While the triplet of parameters a_{ij}, b_{ij} and c_{ij} is referred to as premise parameters or non-linear parameters and they adapt the conditions and the position of the membership function role. Those parameters are corrected during the training mode of procedure by the error back-propagation algorithm. Those premise parameters or nonlinear parameters are updated at each iteration i.e. after each input-output pair is received during training and to minimize the instantaneous error function as given in equation (12),

$$E(n) = \frac{1}{2}(P_M^m(n) - P_A^m(n))^2 \tag{12}$$

Where $P_M{}^m(n)$ is the desired output or supervised output and $P_A{}^m(n)$ is the output of the online CANFIS controller at each step time (n). For each input-output training data pair, the CANFIS operates in the forward pass in order to calculate the current output $P_A{}^m(n)$. Subsequently, going from the output layer, and moving backwards, the error back-propagation executes to calculate the derivatives $\frac{\partial E(n)}{\partial w}$ for each node at every Layer of the network. At the end of every iteration, the non-linear parameter a_{ij}, b_{ij} and c_{ij} of the input membership function is updated by the equation (13) as,

$$\begin{aligned} a_{ij}^{(1)}(n+1) &= \alpha\left(a_{ij}^{(1)}(n)\right) + \eta\left(-\frac{\partial E(n)}{\partial a_{ij}^{(1)}}\right) \\ b_{ij}^{(1)}(n+1) &= \alpha\left(b_{ij}^{(1)}(n)\right) + \eta\left(-\frac{\partial E(n)}{\partial b_{ij}^{(1)}}\right) \\ c_{ij}^{(1)}(n+1) &= \alpha\left(c_{ij}^{(1)}(n)\right) + \eta\left(-\frac{\partial E(n)}{\partial c_{ij}^{(1)}}\right) \end{aligned} \tag{13}$$

Where η is the learning rate of the network parameters and α is the steepest descent momentum constant.

Layer 2 is known as fuzzy AND operation layer. Each node in this layer performs a fuzzy-AND operation. Here, T-norm operator of the algebraic product was chosen. This will result to each node's output. It is the product of all of its inputs and expressed in equation (14). Every input node is connected to that rule node.

$$O_k^{(2)} = w_k = \prod_{i=1}^{k} \prod_{j=1}^{y} O_{ij}^{(1)} \tag{14}$$

Where k =1…n^m. The output of each node in this layer represents the firing strength or the activation value of the corresponding fuzzy rule.

Layer 3 is known as normalization layer. The output of the k^{th} node is the firing strength of each

rule divided by the total sum of the activation values of all the fuzzy rules. This will result in the standardization of the activation value for each fuzzy rule and it is presented in equation (15) as,

$$O_k^{(3)} = \overline{W_k} = \frac{O_k^{(2)}}{\sum_{l=1}^{y^2} O_l^{(2)}} \quad (15)$$

Layer 4 is known as a linear parameter layer. Each node *k* in this layer is accompanied by a set of adjustable parameters d_{1k}^{m}, d_{2k}^{m}… d_{yk}^{m}, d_0^{m} and implements the linear function as expressed in equation (16),

$$O_{km}^{(4)} = \overline{W_k} C_k^m = \overline{W_k}\left(d_{1k}^m I_1^{(1)} + d_{2k}^m I_2^{(1)} + \cdots + d_{yk}^m I_y^{(1)} + d_0^m\right) \quad (16)$$

The weight $\overline{w_k}$ is the normalized activation value of the k^{th} rule, calculated with the aid of equation (15). Adjustable parameters for this layer are called consequent parameters or linear parameters of the CANFIS system and they are set by a recursive least square algorithm. For online supervised CANFIS controller, inputs and output parameters are considered to be G, T and P_A^{m}. The output is expressed in equation (17) as,

$$f^m\left(G(l), T(l)\right) v(l) = P_A^m(l) \quad (17)$$

Where G(l) and T(l) are controller input vectors, f is the known function of the inputs and d(l) is the unknown parameter to be estimated. In order to identify the unknown parameter d(l), we need input-output training data on the target system and it is obtained from the desired model algorithm and expressed in a set of 't' linear equation given in (18) as,

$$f_t^m\left(G(l), T(l)\right) v(l) = P_M^m(l) \quad (18)$$

By the application of recursive least square algorithm, the consequence or linear parameter of the online CANFIS controller is updated in the layer 4. It is given in the equation (19) as,

$$d_{jk_{n+1}}^m = d_{jk_n}^m + \frac{1}{\lambda}\left(P_n - \frac{P_n f^m f^{m^T} P_n}{\lambda + f^{m^T} P_n f^m}\right) * f\left(U - f^{m^T} d_{jk_n}^m\right) \text{ and } d_{0_{n+1}}^m = d_{0_n}^m \quad (19)$$

Where, $P_n = \left(f_t^{m^T} \lambda f_t^m\right)^{-1}$ and λ is the forgetting factor of the online CANFIS controller. The typical value of λ in practice is between 0.9 and 1. The smaller λ is, the faster the effect of old data decay. A small λ sometimes causes numerical instability and thus should be avoided. In this work, λ is taken as 0.9.

Layer 5 is known as output layer. This layer consists of one and only node that produces the network's output as the algebraic sum of the node's inputs [21]. It is presented in equation (20) as,

$$U_a^m = O_m^{(5)} = \sum_{k=1}^{y^2} O_{km}^{(4)} = \sum_{k=1}^{y^2} \overline{W_k} C_k^m = \frac{\sum_{k=1}^{y^2} w_k C_k^m}{\sum_{k=1}^{y^2} w_k} \quad (20)$$

The output of the supervised online CANFIS controller and actual power from PV panel is compared and it is provides the error power value for PI controller and PI controller is providing control current signal to the ZVS and ZCS switching logic generation units. Simulation results and experimental verification of the proposed system is discussed in the subsequent sections of the paper.

5. Simulation results

The proposed supervised online coactive neuro fuzzy inference system based MPPT control algorithm is simulated in MATLAB/Simulink. The PV module is connected to a three stage IBC. The specification of the PV module is shown in Table 1. The I-V and P-V characteristics are shown in Figures.5 (a) &5(b).

Table.1. Parameters of the PV Panel

S.No	Description	Values
1.	Maximum Power	110 Watts
2.	Maximum Voltage	35.5 Volts
3.	Maximum Current	3.2 Amps
4.	Short circuit current	4.35 Amps
5.	Open circuit Voltage	40.5 Volts
6.	Normal operating temperature	25 °C

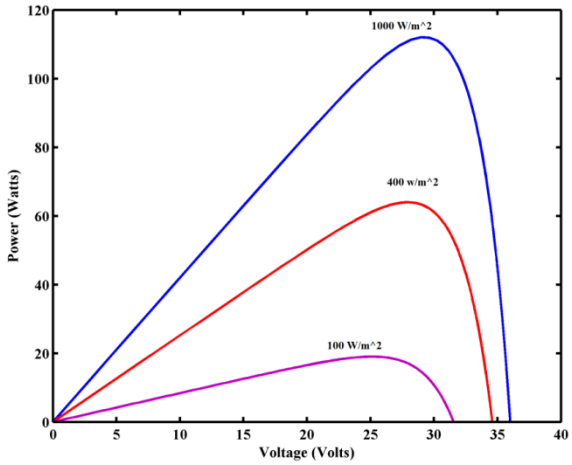

Fig.5. (a) Power versus Voltage characteristics of PV Panel

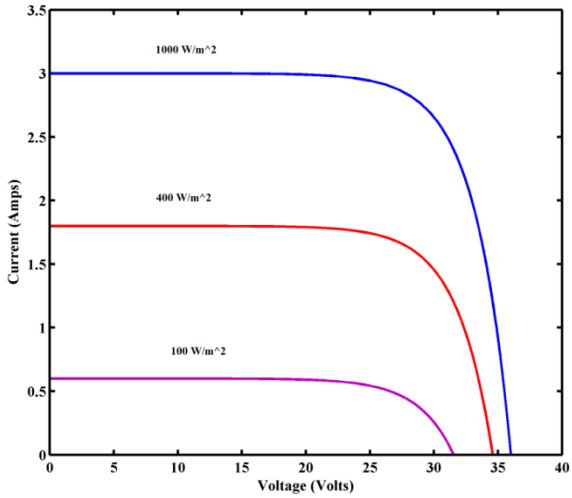

Fig.5. (b) Current versus Voltage characteristics of PV Panel

Simulation studies were carried out under steady state and dynamic conditions with the proposed supervised online CANFIS algorithm and compared with conventional P&O and FLC algorithms respectively.

The input of three-stage IBC is 35 V, the output obtained is about 110 V and the duty cycle of PWM is 33%. The input inductor value is 500 µH, the resonant inductor is 40 µH, the resonant capacitor is 20 nF, the input capacitor is 200 µF and the output capacitor was 440 µF and the load is 30 Ω.

The parameters that are taken to analyze the performance of each MPPT algorithm are transient time, maximum power ratio, oscillation, overshoot and stability. The maximum power ratio is estimated from ratio of the output acquired from simulation work to predictable output obtained in the datasheet of the chosen PV panel which may differ for various irradiances. The noise from the current and voltage sensors are also accounted in the simulation work. The simulink model of the proposed supervised online CANFIS based MPPT algorithm is shown in Figures 5 (c) – 5(d).

5.1. Simulation results with constant irradiance

Steady-state test is performed for various irradiances such as 400, 800 and 1000 W/m^2. Figure 6 shows outcome of each MPPT algorithm towards the MPP and MPPT voltage and the corresponding parameters are tabulated in Table 2.

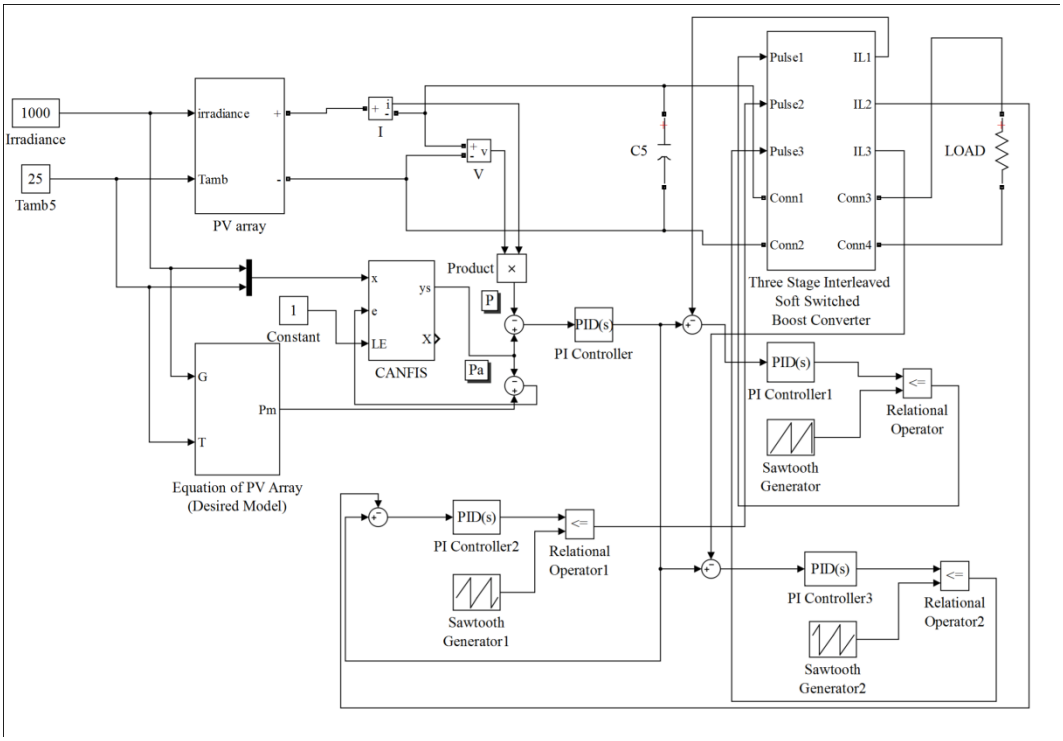

Fig.5. (c) Simulink Model of the proposed MPPT algorithm For PV array

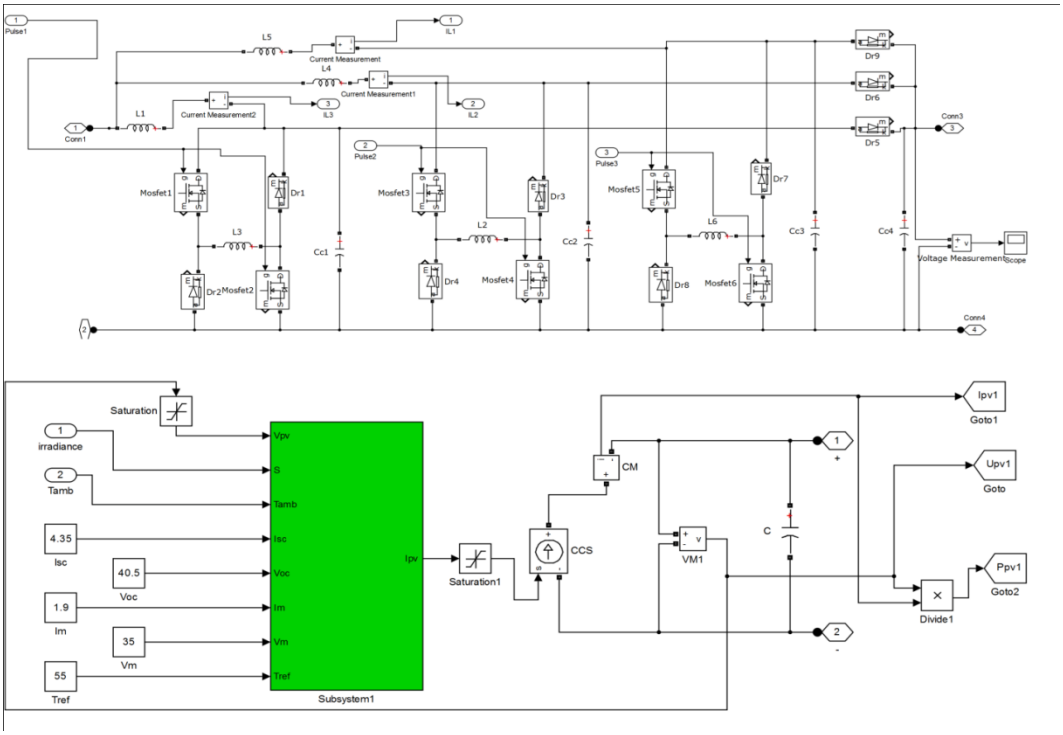

Fig.5. (d) Simulink Model of Three stages soft switched IBC interfaced with PV

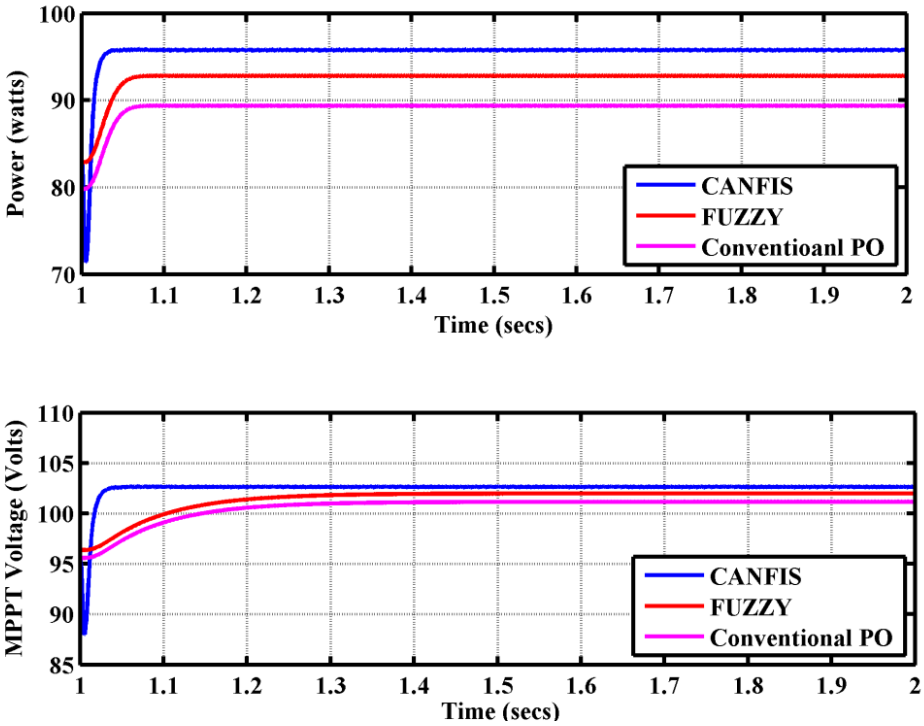

Fig.6. (a) Maximum power and voltage for irradiance 400 W/m^2

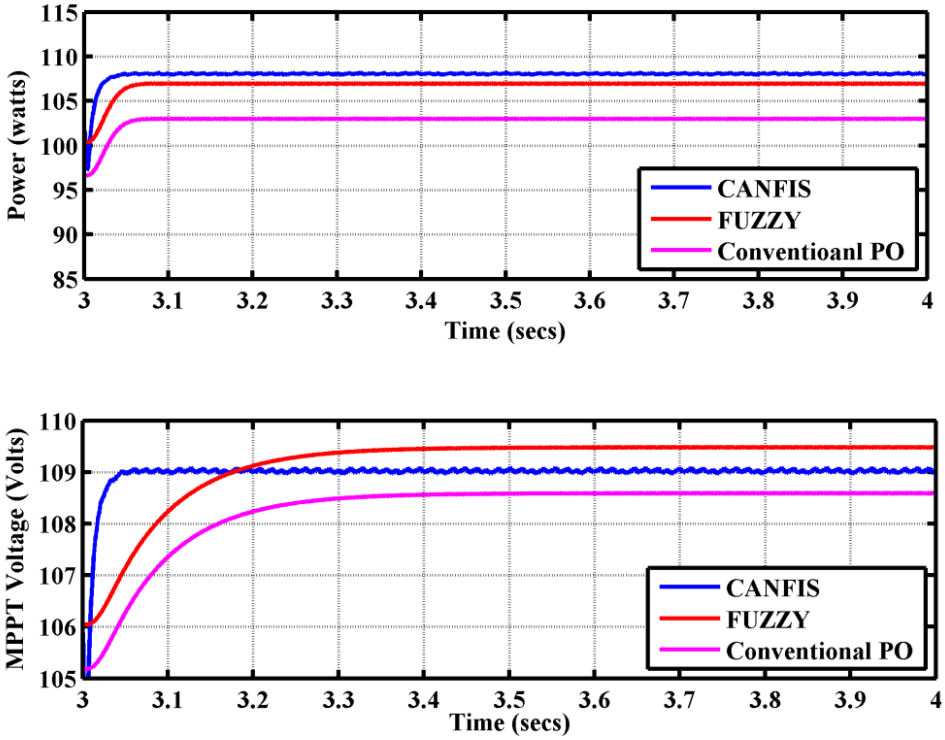

Fig.6. (b) Maximum power and voltage for irradiance 800 W/m^2

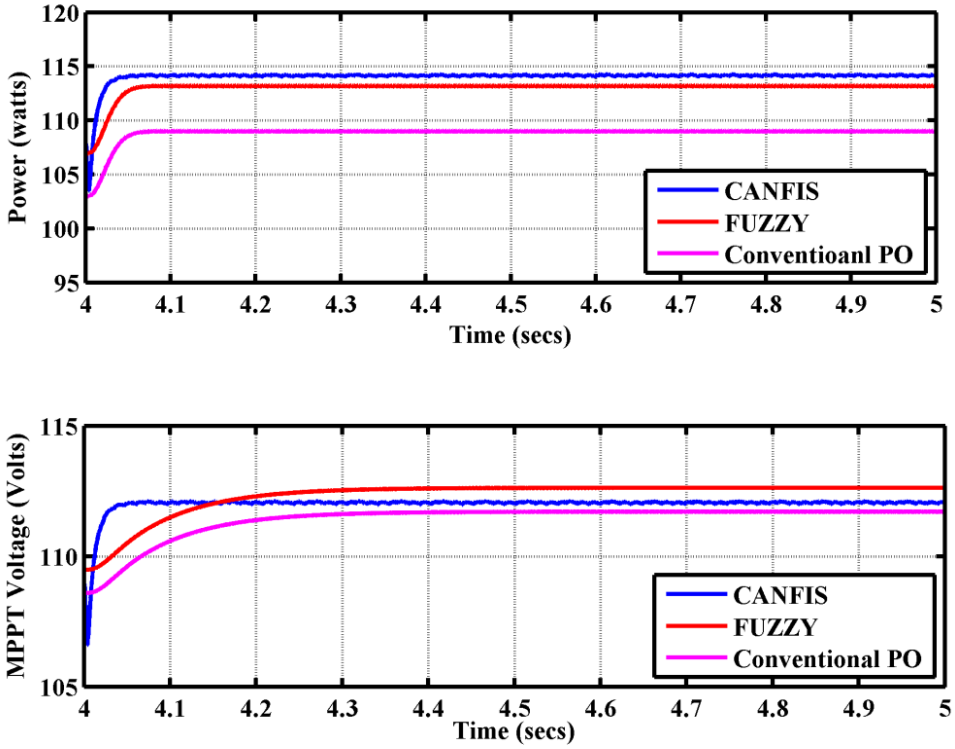

Fig.6. (c) Maximum power and voltage for irradiance 1000 W/m^2

Table.2. Comparison of MPPT algorithm and converter voltage

Comparison results of Maximum Power point									
Irradiance	400 W/m^2			800 W/m^2			1000 W/m^2		
Algorithm	CPO	Fuzzy	CANFIS	CPO	Fuzzy	CANFIS	CPO	Fuzzy	CANFIS
MPP ratio %	89.1	92.1	95.3	90.6	93.1	94.5	89.6	93.5	96.4
Comparison results of converter voltage									
Irradiance	400 W/m^2			800 W/m^2			1000 W/m^2		
Algorithm	CPO	Fuzzy	CANFIS	CPO	Fuzzy	CANFIS	CPO	Fuzzy	CANFIS
Overshoot %	5	2	1	4	3	0.8	4	5.5	0.9
Transient time (msec)	200	200	10	250	200	20	300	200	10

Figure 6 shows the results of all three MPPT algorithms to attain a maximum power point at low irradiance, medium irradiance and high irradiance. At 400 W/m^2 irradiance, proposed algorithm works well at this irradiance as compared to the other two MPPT algorithms. P&O shows the worst dynamic MPP ratio, slow time response and not stable at this condition. High over damped behavior is observed for P&O which may cause power losses. Fuzzy Logic algorithms also produce a low dynamic MPP ratio, slow time response, not that stable and low over damped behavior as compared with proposed algorithm. At 800 W/m^2 irradiance, the figure shows a clear result that confirms supervised online CANFIS produces better performance in terms of the dynamic MPP ratio, stability and time response. P&O algorithm shows the worst performance, especially at this irradiance with low dynamic MPP ratio, high over damped behavior and not that stable. The fuzzy logic algorithm is much better as compared with P&O. At 1000 W/m^2 irradiance, all three MPPT algorithms perform well and produce a high dynamic MPP ratio, good stability and fast time response. In more specific, the supervised online CANFIS algorithm still shows the best performance, especially in term of a dynamic MPP ratio. Performance in low irradiance is critical wherever at this level the power is very small. Both conventional P&O MPPT and fuzzy logic based MPPT algorithms show low capability to extract maximum power when compared to the proposed supervised online CANFIS MPPT algorithm.

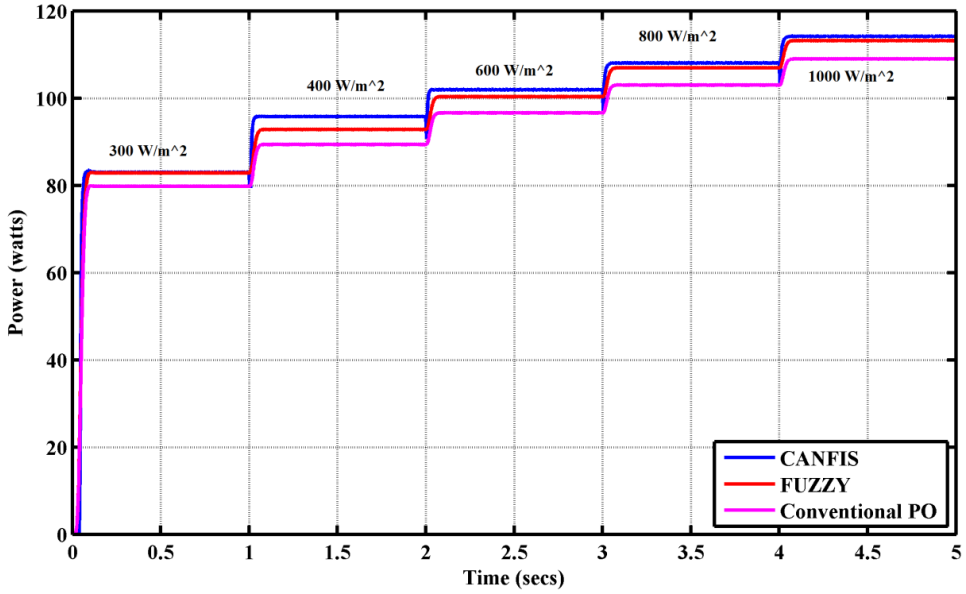

Fig.7. (a) Maximum power point with step change in irradiance level

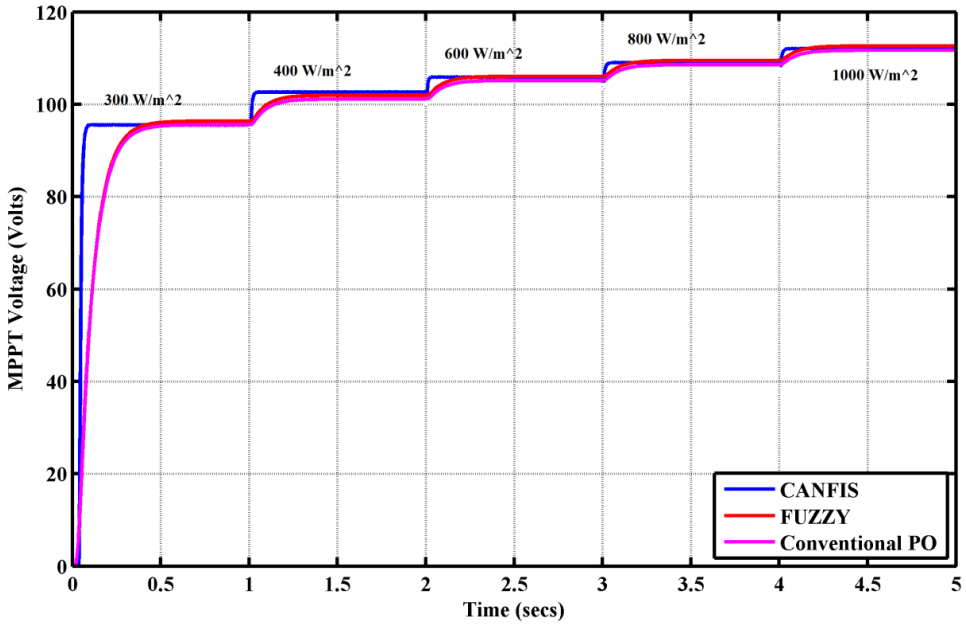

Fig.7. (b) Converter voltage variation with step change in irradiance level

The performance characteristics of three algorithms are shown in Table 2. For P&O algorithm, the time response is about 200-300 ms before reaching to stable state, overshoot is about 4-5.5 %, power ratio is about 89.1-90.6 % and high oscillation exists. For FLC algorithm, the time response is about 200 ms before reaching stable state, overshoot is about 2-5.5 %, power ratio is about 92.1-93.5 % and high oscillation is observed. The best result is from supervised online CANFIS algorithm that achieves time response at only 10-20 ms before reaching stable state, overshoot is about 0.8-1 %, power ratio is about 94.5-96.4 and only low oscillation exists. Therefore, from the simulation results, performance of proposed algorithm is much better as compared to both conventional P&O and Fuzzy logic MPPT algorithms in terms of time response, overshoot, maximum power ratio, oscillation and stability.

5.2. Simulation results with step varying irradiance

Figure 7 shows the maximum power point and converter voltage variation with step change in

irradiance level of PV panel. Figure 7 (a) shows the maximum point tracking response for step change in irradiance level. From these results, all MPPT algorithms are able to extract Maximum power point of the PV module. When the irradiation is about 0–400 W/m^2, the conventional P&O not able to extract the maximum power due to power losses and also it is noticed that the slowest time response, high oscillation and not that stable. The Fuzzy Logic MPPT algorithm shows better results when compared with conventional P&O in terms of good time response, low oscillation and stable. However, the supervised online CANFIS algorithms truly show the most excellent performance when compared with both conventional P&O and fuzzy logic MPPT algorithms. The efficiency is very high, time response is quick, really small oscillation exists and operation is more stable.

Figure 7 (b) shows variation of converter voltage with step change in irradiance level. Three MPPT algorithms start to work and boost up the output voltage from 85 V to 110 V according with irradiance level. The major differences between these three algorithms are their effects on time response and overshoot. For P&O algorithm, the time response is around about 300 ms before reaching to stable state, overshoot is around about 10V and high oscillation exists. For FLC algorithm, the time response is around 200 ms before reaching stable state, overshoot is around 5V and high oscillation is observed. For the proposed supervised online CANFIS MPPT algorithm the time response is about 15ms before reaching stable state, overshoot is around about 1V and only low oscillation exists. Therefore, the proposed CANFIS algorithm is much better compared to P&O and fuzzy logic MPPT algorithms in terms of overshoot, time response, oscillation, maximum power ratio and stability.

6. Experimental setup and results

In order to validate the proposed supervised online CANFIS MPPT algorithm experimental laboratory setup is developed and it is shown in Figure 8 (a). The three stage interleaved soft switched boost converter is also fabricated. TMS320LF2407A DSP Processor board is used to implement the MPPT algorithm [22].

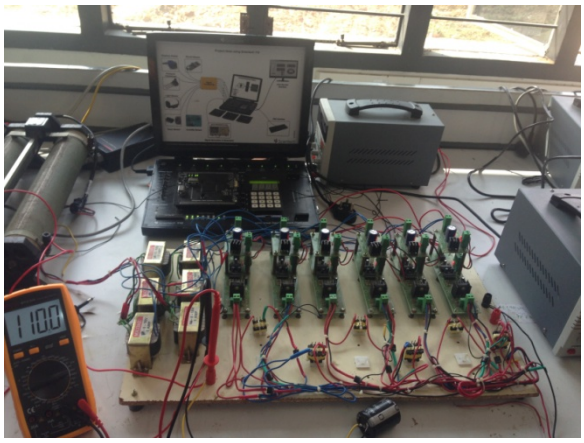

Fig.8. (a) Real time experimental setup of proposed control system

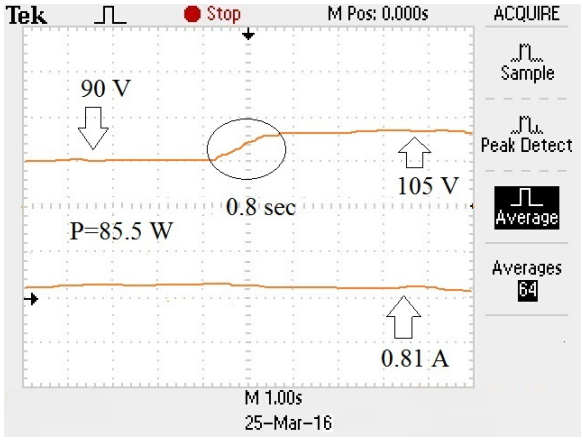

Fig.8. (b) Time response of output voltage and current for conventional P&O MPPT algorithm

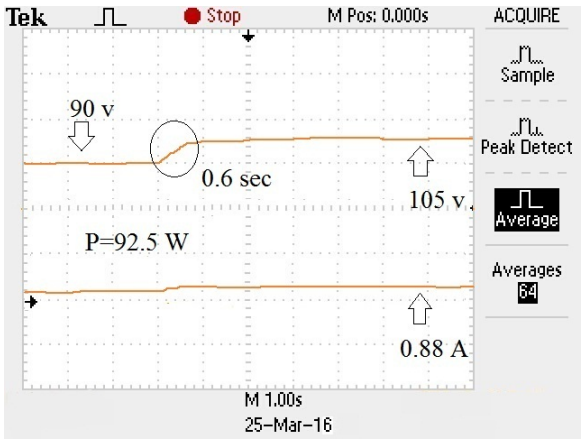

Fig.8. (c) Time response of output voltage and current for Fuzzy logic MPPT algorithm

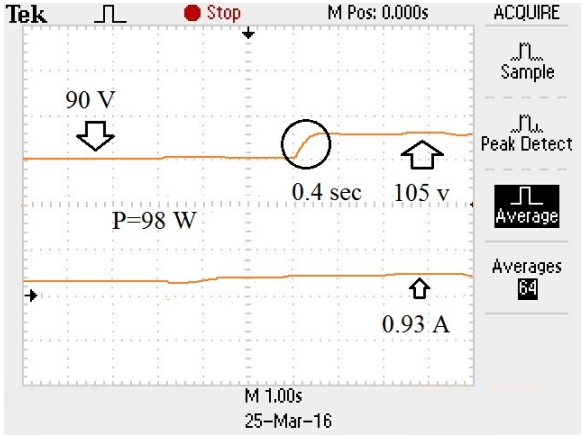

Fig.8. (d) time response of output voltage and current for supervised online CANFIS MPPT algorithm

Time responses of the output current and voltage with all three MPPT algorithms are shown in Figures 8 (b)-(d). Voltage of three stage soft switched IBC is boosted from 90V to 105V. The proposed MPPT algorithm shows the fastest transient response and the response time is around 400 ms, whereas for Fuzzy MPPT it is about 600 ms, and the P&O algorithm is about 800 ms. Maximum power point is 98W for proposed algorithm, fuzzy logic is around 92.5W and for conventional P&O is about 85.5W. Thus the experimental results are verified with the simulation results. From the simulation and experimental results, it is clear that the proposed supervised online CANFIS MPPT algorithm performs well in all aspects for tracking maximum power from PV which will be more suitable for all applications.

7. Conclusion

A novel supervised online CANFIS based maximum power point technique for photovoltaic system has been presented. The overall photovoltaic conversion system has been designed and simulated in MATLAB/Simulink. Effectiveness of the proposed MPPT is analyzed and compared with conventional P&O and Fuzzy Logic control. The performance of the photovoltaic system is simulated for various operating conditions with proposed technique to suit the real time environment. In order to formulate a realistic comparison, several performance measures are used such as maximum power ratio, overshoot and transient time. The results obtained from the simulations clearly show the drastic improvements on performance measures and extract maximum power from PV panel than other considered techniques i.e., maximum power ratio is around 96 %, transient time response is less than 15 ms, overshoot is less than 1 % and more stable than conventional P&O and fuzzy logic MPPT algorithm. And also the proposed controller was implemented with TMS320LF2407A DSP Processor and tested for different irradiance level. From the results, it is ascertained that, the proposed MPPT algorithm performs very well in all aspect than the other considered MPPT algorithm.

References

1. S. R. Bull: *Renewable energy today and tomorrow.* In: Proceedings of the IEEE conference, (2001), Vol. 89, No. 8, pp. 1216-1226.
2. Geury, Thomas, Pinto, Sonia, Gyselinck, Johan: *Current source inverter-based photovoltaic system with enhanced active filtering functionalities.* In: IET Power Electronics, (2015), Vol.8, No.12, pp.2483-2491.
3. V. Salas, E. Olías, A. Barrado, A. Lázaro: *Review of the maximum power point tracking algorithms for stand-alone photovoltaic systems.* In: Solar Energy Materials and Solar Cells, (2006), Vol.90, No.11, pp.1555-1578.
4. K.Ishaque, Z.Salam: *A review of maximum power point tracking techniques of PV system for uniform insulation and partial shading condition,* In: Renewable and Sustainable Energy Reviews. (2013), Vol.19, pp. 475–488.
5. I.Houssamo, F.Locment, M.Sechilariu: *Maximum power tracking for photovoltaic power system: development and experimental comparison of two algorithms*. In: Renewable Energy, (2010), Vol.35, pp. 2381–2387.
6. Ali Reza Reisi, Mohammad Hassan Moradi, Shahriar Jamasb: *Classification and comparison of maximum power point tracking techniques for photovoltaic system: A review*. In: Renewable and Sustainable Energy Reviews, (2013), Vol.19, pp. 433-443.
7. I.Houssamo, F.Locment, M.Sechilariu: *Experimental analysis of impact of MPPT methods on energy efficiency for photovoltaic power systems*, In: International Journal Electrical and Power Energy System. (2013),Vol. 46, pp. 98–107.
8. N. Femia, G. Petrone, G. Spagnuolo and M. Vitelli: *Optimization of perturb and observe maximum power point tracking method*. In: IEEE

Transactions on Power Electronics,(2005), Vol. 20, No. 4, pp. 963-973.

9. S. K. Kollimalla and M. K. Mishra: *A Novel Adaptive P&O MPPT Algorithm Considering Sudden Changes in the Irradiance*. In: IEEE Transactions on Energy Conversion, (2014), Vol. 29, No.3, pp. 602-610.
10. J.Surya Kumari, C.h.Sai Babu, A.Kamalakar Babu: *Design and analysis of P&O and IP&O MPPT techniques for photovoltaic system*, In: International Journal of Modern Engineering and Research, (2012), Vol.2, No.4, pp. 2174–2180.
11. M.G.Villalva, J.R.Gazoli, E.R.Filho: *Analysis and simulation of the P&O algorithm using a linearized PV Array Model*. In: Industrial Electronics Conference, (2009), pp. 231–236.
12. Algazar, M.M., AL-monier, H., Abd EL-halim, H., El Kotb Salem, M. E.: 'Maximum power point tracking using fuzzy logic control', Electr. Power Energy Syst., 2012, 39, pp. 21–28.
13. N.Khaehintung, P.Sirisuk, W.Kurutach: *A novel ANFIS controller for maximum power point tracking in photovoltaic systems*. In: Proceeding of Fifth International Conference on Power Electronics and Drive Systems, (2003), Vol. 2, pp.833–836.
14. A.Iqbal, H.Abu-Rub, Sk.M.Ahmed: *Adaptive neuro-fuzzy inference system based maximum power point tracking of a solar PV module*. In: IEEE International conference on Energy, (2010), pp.51–56.
15. M.G. Villalva, J.R. Gazoli, E.R. Filho: *Comprehensive approach to modeling and simulation of photovoltaic arrays*. In: IEEE Transaction on Power Electron , (2009), Vol.5 , pp.1198 – 1208.
16. Chikh, Ali, Chandra, Ambrish: *Adaptive neuro-fuzzy based solar cell model*. In: IET Renewable Power Generation, (2014), Vol.8, No.6, pp. 679-686.
17. T. Bennett, A.Zilouchian, R.Messenger: *Photovoltaic model and converter topology considerations for MPPT purposes*. In: Solar Energy, (2012), Vol.86, pp. 2029–2040.
18. Freitas, Antônio Alisson Alencar; Tofoli, Fernando Lessa; Sá Júnior, Edilson Mineiro; Daher, Sergio; Antunes, Fernando Luiz Marcelo: *High-voltage gain dc–dc boost converter with coupled inductors for photovoltaic systems*. In: IET Power Electronics, (2015),Vol.8, No.10, pp. 1885-1892.
19. E Silva Aquino, Ranoyca Nayana Alencar Leão, Tofoli, Fernando Lessa, Praca, Paulo Peixoto, Oliveira, Demercil de Souza Jr, Barreto, Luiz Henrique Silva Colado: *Soft switching high-voltage gain dc–dc interleaved boost converter*. In: IET Power Electronics, (2015), Vol.8, No.1, pp. 120-129.
20. Luo, Quan-ming; Yan, Huan; Chen, Si; Zhou, Luo-wei: *Interleaved high step-up zero-voltage-switching boost converter with variable inductor control*. In :IET Power Electronics, (2014), Vol.7, No.12, pp. 3083-3089.
21. Nguyen Quoc Dinh, Nitin V. Afzulpurkar: *Neuro-fuzzy MIMO nonlinear control for ceramic roller kiln*. In: Simulation Modelling Practice and Theory, (2007), Vol. 15, No.10, pp. 1239-1258.
22. Demirtas, M.: *DSP-based sliding mode speed control of induction motorusing neuro-genetic structure*. In: Expert System and Application, (2009), Vol.36, No.3, pp. 5533–5540.